UNIVERSITÉ DE GENÈVE

Archive ouverte UNIGE
https://archive-ouverte.unige.ch

Article scientifique | Article | 2016

Published version | Open Access

This is the published version of the publication, made available in accordance with the publisher's policy.

Mutations in the MOV10L1 ATP Hydrolysis Motif Cause piRNA Biogenesis Failure and Male Sterility in Mice

Fu, Qi; Pandey, Radha Raman; Leu, N. Adrian; Pillai, Ramesh; Wang, Jeremy P.

How to cite

FU, Qi et al. Mutations in the MOV10L1 ATP Hydrolysis Motif Cause piRNA Biogenesis Failure and Male Sterility in Mice. In: Biology of reproduction, 2016, vol. 95, n° 5, p. 1–7. doi: 10.1095/biolreprod.116.142430

This publication URL: https://archive-ouverte.unige.ch/unige:175086

Publication DOI: 10.1095/biolreprod.116.142430

© The author(s). This work is licensed under a Creative Commons Attribution-NonCommercial (CC BY-NC 4.0) https://creativecommons.org/licenses/by-nc/4.0

BIOLOGY OF REPRODUCTION (2016) **95**(5):103, 1–7
Published online before print 21 September 2016.
DOI 10.1095/biolreprod.116.142430

Mutations in the MOV10L1 ATP Hydrolysis Motif Cause piRNA Biogenesis Failure and Male Sterility in Mice[1]

Qi Fu,[3] Radha Raman Pandey,[4] N. Adrian Leu,[3] Ramesh S. Pillai,[4] and P. Jeremy Wang[2,3]

[3]*Department of Biomedical Sciences, University of Pennsylvania School of Veterinary Medicine, Philadelphia, Pennsylvania*
[4]*Department of Molecular Biology, University of Geneva, Geneva, Switzerland*

ABSTRACT

Piwi-interacting RNAs (piRNAs) are a class of small noncoding RNAs. piRNAs protect the genome integrity of the germline by silencing active transposable elements and are essential for germ cell development. Most piRNA pathway proteins are evolutionarily conserved. MOV10L1, a testis-specific RNA helicase, binds to piRNA precursors and is a master regulator of piRNA biogenesis in mouse. Here we report that mutation of the MOV10L1 ATP hydrolysis site leads to depletion of piRNAs on Piwi proteins, de-repression of transposable elements, and conglomeration of piRNA pathway proteins into polar granules. The *Mov10l1* mutant mice exhibit meiotic arrest and male sterility. Our results show that mutation of the MOV10L1 ATP hydrolysis site perturbs piRNA biogenesis.

male fertility, meiosis, MOV10L1, piRNA, retrotransposon

INTRODUCTION

Piwi-interacting RNAs (piRNAs) are a unique class of small noncoding RNAs (nucleotides [nt] 23–31) with a preference for a 5′ uridine nucleotide. piRNAs are expressed predominantly in the germline of metazoan species including Caenorhabditis elegans, Drosophila, zebrafish, and mouse [1–6]. piRNAs associate with Piwi proteins and guide Piwi proteins to cleave and silence active transposable elements (TE) [7]. piRNAs are also required for proper germ cell development and fertility [7]. In mouse, piRNAs are required only for spermatogenesis [8, 9]. Two populations of piRNAs are generated during mouse spermatogenesis, pre-pachytene piRNAs and pachytene piRNAs.

Pre-pachytene piRNAs are enriched in TE-derived sequences and associate with the Piwi proteins MILI (gene symbol: *Piwil2*) and MIWI2 (*Piwil4*) in gonocytes and spermatogonia [10–12]. Most pre-pachytene piRNAs are expressed prenatally in gonocytes. Pre-pachytene piRNAs are required for DNA methylation and repression of the retrotransposons LINE1 and IAP [10–15]. Loss of pre-pachytene piRNA biogenesis/loading onto Piwi proteins results in meiotic arrest at the zygotene stage of meiosis I [13, 16–23]. It is generally accepted that de-repression of TE causes massive DNA damage in spermatocytes, which activates the meiotic checkpoint and thus meiotic arrest in spermatocytes [24, 25].

Pachytene piRNAs are expressed postnatally in pachytene spermatocytes and round spermatids. They associate with the Piwi proteins MILI and MIWI (*Piwil1*) and constitute 95% of known piRNAs [4, 5, 26]. Most pachytene piRNAs are derived from intergenic regions [4, 5, 26]. The precise functions of pachytene piRNAs are still unclear. Recent studies have implicated pachytene piRNAs in the cleavage of meiotic and postmeiotic messenger RNAs [27–29]. Although pachytene piRNAs are not enriched for TE-derived sequences, MILI-bound and MIWI-bound pachytene piRNAs are required to silence LINE1 elements in pachytene spermatocytes and in round spermatids, respectively [5, 30, 31]. Loss of pachytene piRNA biogenesis/loading onto Piwi proteins results in round spermatid arrest [32, 33].

Studies of mammalian piRNAs have provided a framework for how piRNAs are generated and have identified a plethora of components in the piRNA pathway; however, many of the mechanisms involved remain unclear. Most components of the piRNA pathway are compartmentalized in nuages, electron-dense compartments in the cytoplasm of germ cells [16, 22, 34–36]. piRNA pathway components localize to two distinct, adjacent nuages in fetal germ cells, the pi-body and piP-body [35]. In spermatogonia and spermatocytes, the piRNA pathway is compartmentalized in the nuages localized among mitochondrial clusters, collectively termed the intermitochondrial cement [34]. In postmeiotic germ cells, the piRNA pathway components are compartmentalized in a large single nuage termed the chromatoid body [36]. Pre-pachytene and pachytene piRNAs are initially generated through primary biogenesis. During primary biogenesis, piRNA precursor transcripts are cleaved by the endonuclease PLD6 and loaded onto MILI and MIWI as piRNA intermediates [7, 37–39]. Like mature piRNAs, piRNA intermediates also contain a preference for a 5′ uridine nucleotide [39]. In the final steps of primary biogenesis, PNLDC1, a 3′–5′ exonuclease termed Trimmer, interacts with TDRKH/Papi to trim piRNA intermediates at their 3′ ends [40, 41]. Trimmed piRNAs are 2′-*O*-methylated at their 3′ ends by HENMT1 [42]. Additionally, repeat-derived pre-pachytene piRNAs are amplified through the ping-pong cycle [12]. The pre-pachytene piRNAs guide MILI to cleave complementary RNA transcripts that are loaded onto either MILI or MIWI2 and processed to generate antisense (secondary) piRNAs [15]. Secondary piRNAs contain a signature adenosine at the 10th nucleotide [12]. MILI-bound secondary piRNAs cleave complementary RNA transcripts to amplify the initial piRNAs [15]. MIWI2-bound secondary piRNAs guide MIWI2 into the nucleus where MIWI2 is

[1]Supported by U.S. National Institutes of Health grant R01HD069592 to P.J.W.
[2]Correspondence: P. Jeremy Wang, Department of Biomedical Sciences, University of Pennsylvania School of Veterinary Medicine, 3800 Spruce Street, Philadelphia, PA 19104. E-mail: pwang@vet.upenn.edu

Received: 3 June 2016.
First decision: 13 July 2016.
Accepted: 19 September 2016.
© 2016 by the Society for the Study of Reproduction, Inc. This article is available under a Creative Commons License 4.0 (Attribution-Non-Commercial), as described at http://creativecommons.org/licenses/by-nc/4.0
eISSN: 1529-7268 http://www.biolreprod.org
ISSN: 0006-3363

hypothesized to recruit DNA methylation machinery to silence active LINE1 elements [11–13].

MOV10L1 is a testis-specific RNA helicase required for both pre-pachytene and pachytene piRNA biogenesis [16, 33]. MOV10L1 interacts with MILI, MIWI, and TDRD1 and directly binds to piRNA precursors near regions with a high propensity to form secondary structures such as G-quadruplexes [16, 43]. MOV10L1 binding to piRNA precursors precedes the loading of precursors onto MILI and MIWI [43]. Postnatal deletion of *Mov10l1* resulted in an accumulation of pachytene piRNA precursors [33]. A mouse knockin mutant containing a point mutation in the conserved ATP binding motif of the MOV10L1 RNA helicase domain also exhibited an accumulation of pre-pachytene piRNA precursors [43]. These studies support the function of MOV10L1 as an RNA helicase during primary biogenesis to recognize and resolve secondary structures within piRNA precursors, allowing the piRNA precursor to be processed into piRNA intermediates. To further explore the requirement for MOV10L1 RNA helicase activity in piRNA biogenesis, we generated a mouse knockin mutant containing mutations in the conserved ATP hydrolysis motif of the MOV10L1 RNA helicase domain. Analysis of this mouse model shows that the ATP-binding activity of MOV10L1 is not sufficient for piRNA biogenesis and that mutations in its ATP hydrolysis site also abolish piRNA biogenesis.

MATERIALS AND METHODS

Mouse Breeding

Mice were housed in a barrier vivarium, monitored daily and under veterinarian care by the attending veterinarians from University Laboratory Animal Resources at the University of Pennsylvania. All experimental protocols were approved by the Institutional Animal Care and Use Committee of the University of Pennsylvania.

Generation of the Mov10l1 *DE888AA Knockin Allele*

The 7.4-kb targeting construct contains a neomycin selection cassette (1.87-kb) flanked by left (2.88-kb) and right arms (2.65-kb) homologous to exons 18–22 of *Mov10l1*. The left arm contains mutations from GAC GAG (aspartic acid glutamic acid, respectively) to GCG GCG (alanine alanine) corresponding to codons 888 and 889 (exon 20) of *Mov10l1*. To generate the *Mov10l1* knockin targeting construct, the left arm and right homologous arms were amplified from a *Mov10l1*-containing a BAC clone (RP23-269F24) by high-fidelity PCR. Codons 888 and 889 were mutated by PCR-based mutagenesis. The neomycin selection cassette was flanked by *loxP* sites for Cre-mediated removal. The targeting construct was sequenced to confirm the mutations and linearized by digestion using *Cla*I. The V6.5 hybrid embryonic stem (ES) cells were electroporated with the linearized targeting construct and cultured in the presence of 350 μg/ml G418. Of the 392 G418-resistant ES clones that were screened for homologous recombination, four targeted clones were obtained. One clone was injected into blastocysts and yielded germline transmission of the *Mov10l1* knockin allele. The neomycin selection cassette was removed by crossing *Mov10l1*$^{KI/+}$ mice with *Actb*-Cre mice that express Cre ubiquitously [44]. All studies were performed with mice without the neomycin cassette. The wild-type (480 bp) and knockin (598 bp) alleles were assayed by PCR with primers forward: GCCAGGTAAGGCCTGTGTCTT and reverse: GCCTAGT GACTGAAAGGAGGGA. PCR primers flanked the remaining *loxP* site and adjacent vector sequence.

Antibodies

The following primary antibodies were used: MOV10L1 [16], MILI (catalog no. ab36764; Abcam) [45], ACTB (catalog no. A5441; Sigma-Aldrich), MIWI2 [12, 46]), LINE1 ORF1p [47], and IAP GAG [48]. The same LINE1 ORF1p antibody was previously used for immunofluorescence in other studies [16, 17, 21, 22]. The same IAP GAG antibody was used for immunofluorescence in other studies [16, 22]. The LINE1 ORF1p and IAP GAG antibodies were previously validated by Western blot analyses [16]. For Western blot analysis, testicular protein lysates were subjected to 8% SDS-PAGE, blotted, and probed with antibodies.

Histology and Immunofluorescence

For histology, testes were fixed in Bouin solution overnight, dehydrated in a series of ethanol washes, embedded in paraffin, sectioned, and stained with hematoxylin and eosin. Anti-MOV10L1 (affinity purified, 1:5 dilution), anti-MILI (1:100 dilution; Abcam), anti-MIWI2 (1:500 dilution), anti-LINE1 ORF1p (1:1000 dilution), and anti-IAP GAG (1:5000 dilution) were used as primary antibodies for immunofluorescent staining. Immunofluorescence was performed using frozen sections of testes fixed in 4% paraformaldehyde for 3 h at 4°C. Sections were blocked for 1 h at room temperature with a buffer containing 10% goat serum. Sections were then incubated with the primary antibody for 1 h at 37°C. The blot was washed three times and incubated with a fluorescein secondary antibody (Vector Laboratories) (1:100 dilution) for 1 h at room 37°C. Sections were washed three times. DNA was stained with 4′,6-diamidino-2-phenylindole (DAPI).

Immunoprecipitation and Detection of piRNAs

Affinity-purified anti-MILI [45] and anti-MIWI2 (crude serum from rabbit) [46] were bound to protein G-Sepharose 4 Fast Flow beads (GE Healthcare) and used to purify MILI and MIWI2 complexes from embryonic mouse testis extracts (50 mM Tris, pH 8, 150 mM NaCl, 5 mM MgCl2, 10% glycerol, 1 mM dithiothreitol [DTT], 0.5% sodium deoxycholate [Sigma], 1% Triton X-100, 1 tablet of complete protease inhibitor [Roche] per 5 ml, 2 mM vanadyl ribonucleoside complex [Sigma]). After five washes (10 mM Tris, pH 8, 150 mM NaCl, 0.05% [v/v] nonyl phenoxypolyethoxylethanol [NP-40]), the retained proteins in RNA complexes were digested by proteinase K (42°C, 30 min), and finally associated RNA were isolated by phenol chloroform extraction and precipitated in ethanol. To visualize RNAs, they were dephosphorylated with rAPid alkaline phosphatase (recombinant bovine phosphatase; Roche) and 5′-end labeled with γ-[^{32}P]ATP with T4 polynucleotide kinase (Thermo Scientific). The labeled RNAs were resolved by 15% (w/v) urea-PAGE. Gels were exposed to Phosphor Storage screens (GE Health) and scanned (Typhoon scanner; GE Health).

Analysis of Mov10l1 *and* Actb *Expression*

Total RNA was extracted from testes using Trizol reagent (Invitrogen), treated with DNase I (Invitrogen), and reverse transcribed to cDNA, using M-MLV reverse transcriptase (Promega) according to the manufacturer's instructions. *Mov10l1* expression was assayed by PCR with the primers GGAAAGACTGTGACTATAATCGAGG and CCTCACTCCATGGAA GATGAGAG. *Actb* expression was assayed by PCR with the primers GCGTGACATCAAAGAGAAGCT and CTTGATCTTCATGGTGCTAGG.

RESULTS

Generation of a Mov10l1 *Knockin Allele Harboring Mutations in the MOV10L1 ATP Hydrolysis Motif*

MOV10L1 is a member of the Superfamily I of DNA/RNA helicases [43, 49]. The RNA helicase activity of this superfamily is dependent on their ATP binding and ATP hydrolysis activities. Mutation of conserved residues in the ATP hydrolysis site of UPF1, one of the closest homologs of MOV10L1, ablated UPF1 RNA helicase activity [50]. UPF1 is required for nonsense-mediated decay. Intriguingly, dissociation of the UPF1:RNA complex depends on ATP binding but not ATP hydrolysis. The MOV10L1 RNA helicase domain is located at its C-terminal region and contains two RecA-like domains (Fig. 1A) [51]. The first RecA-like domain harbors Walker A (ATP binding) and Walker B (ATP-hydrolysis) motifs [52]. To examine the requirement for MOV10L1 ATP hydrolysis activity during piRNA biogenesis, we generated a *Mov10l1* knockin allele by mutating two conserved residues (DE888.889AA) within the ATP hydrolysis motif of the MOV10L1 RNA helicase domain (Fig. 1B) [50, 52].

The *Mov10l1*$^{KI/+}$ mice were viable and fertile, suggesting that the mutation is not dominant negative. We examined the expression of MILI and MOV10L1 in the testes of *Mov10l1*$^{KI/+}$

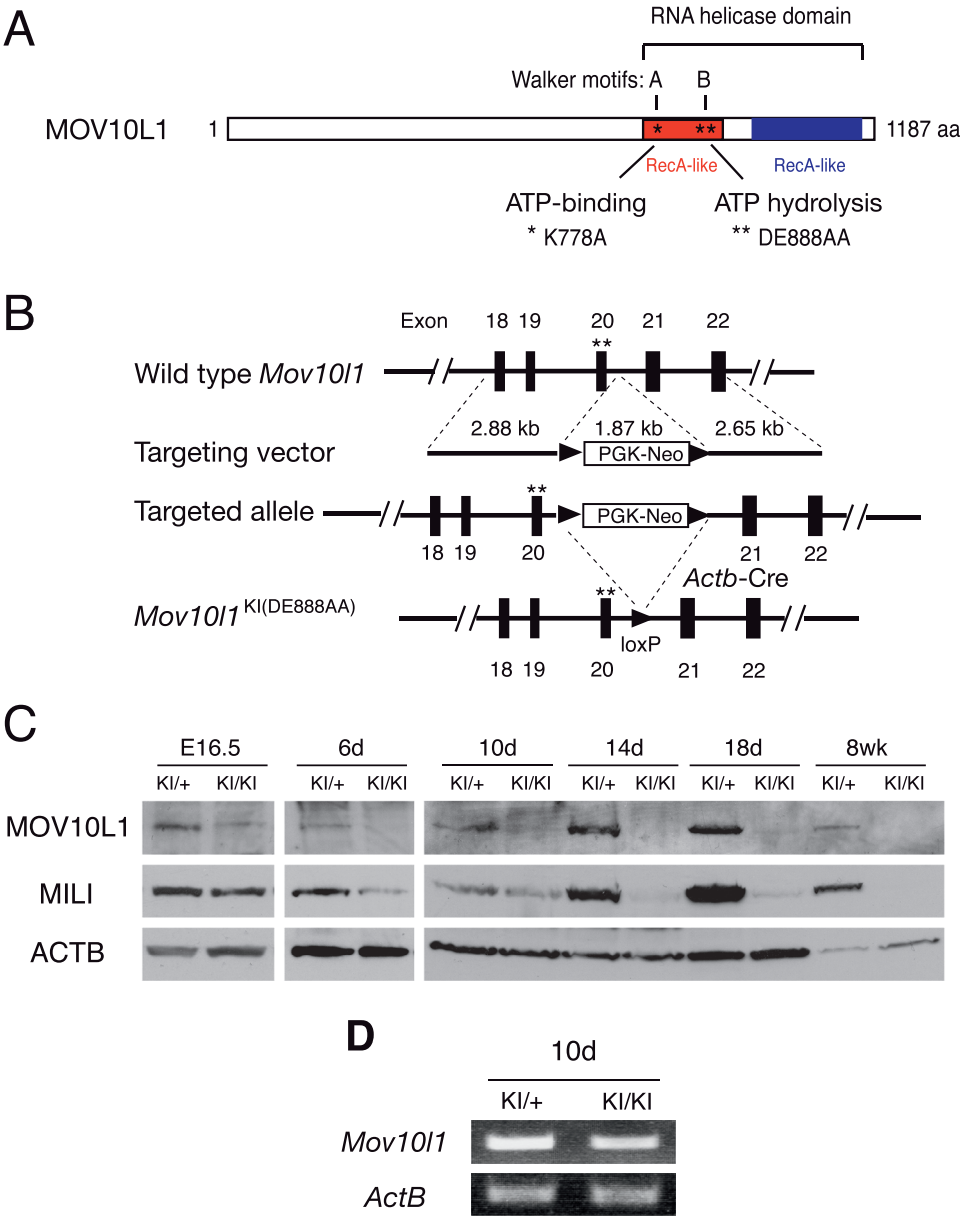

FIG. 1. Generation and expression of the *Mov10l1* knockin allele with mutations in its ATP hydrolysis site. **A**) The RNA helicase domain of the MOV10L1 protein is shown. *ATP-binding (Walker A) and **ATP hydrolysis (Walker B) motifs. K(778) and D(888)E(889) are critical residues. The K778A knockin mutation was previously reported [43]. **B**) Generation of the *Mov10l1* knockin (DE888.889AA) allele. The neo selection cassette is flanked by *loxP* sites and is removed by *Actb*-Cre. *Position of the DE → AA mutation in *Mov10l1*. **C**) Western blot analysis of MOV10L1 in testes from E16.5, Postnatal Day 6 (6d), 10d, 14d, and 18d and 8 wk-old $Mov10l1^{KI/+}$ and $Mov10l1^{KI/KI}$ mice. ACTB serves as loading control. **D**) Semiquantitative RT-PCR analysis of *Mov10l1* and *Actb* transcript abundance in testes from 10-day-old $Mov10l1^{KI/+}$ and $Mov10l1^{KI/KI}$ mice. Total RNAs were pretreated with DNase I. RT-PCR produced no products in controls without reverse transcriptase (data not shown).

and $Mov10l1^{KI/KI}$ mice at embryonic and various postnatal stages of development (Fig. 1C). Both the MILI and MOV10L1 proteins were present in testes from $Mov10l1^{KI/+}$ mice at all ages. MILI was readily detectable in the testes of $Mov10l1^{KI/KI}$ mice from Embryonic Day 16.5 (E16.5) through Postnatal Day 10 and were still detectable at Days 14 and 18. Mutant MOV10L1 protein was present in the testes of $Mov10l1^{KI/KI}$ mice at E16.5 but at a reduced level compared to the testes of $Mov10l1^{KI/+}$ mice (Fig. 1C). However, mutant MOV10L1 protein was not detected in the testes of $Mov10l1^{KI/KI}$ mice at Postnatal Day 6 and beyond (Fig. 1C). We also examined *Mov10l1* transcript in the testes of 10-day-old $Mov10l1^{KI/+}$ and $Mov10l1^{KI/KI}$ mice. The *Mov10l1* transcript level in $Mov10l1^{KI/KI}$ mice was comparable to that in $Mov10l1^{KI/+}$ mice (Fig. 1D). These results show that the MOV10L1 mutant protein was present in embryonic germ cells but reduced in postnatal $Mov10l1^{KI/KI}$ germ cells, likely due to decreased protein stability.

Mov10l1$^{KI/KI}$ *Males Exhibit Meiotic Arrest and Sterility*

$Mov10l1^{KI/KI}$ mice were viable with no apparent gross abnormalities. The fertility of $Mov10l1^{KI/KI}$ mice was sexually dimorphic: males were sterile, but females were fertile. The body weight of 6-wk-old $Mov10l1^{KI/KI}$ mice (21 ± 0.9 g) was similar to that of their heterozygous littermates (22.21 ± 1.9 g) ($P = 0.1$). However, the testis weight of 6-wk-old $Mov10l1^{KI/KI}$ mice (58 ± 5 mg) was 37% of that of their heterozygous littermates (155 ± 14 mg) ($P = 0.001$, Student *t*-test) (Fig. 2A).

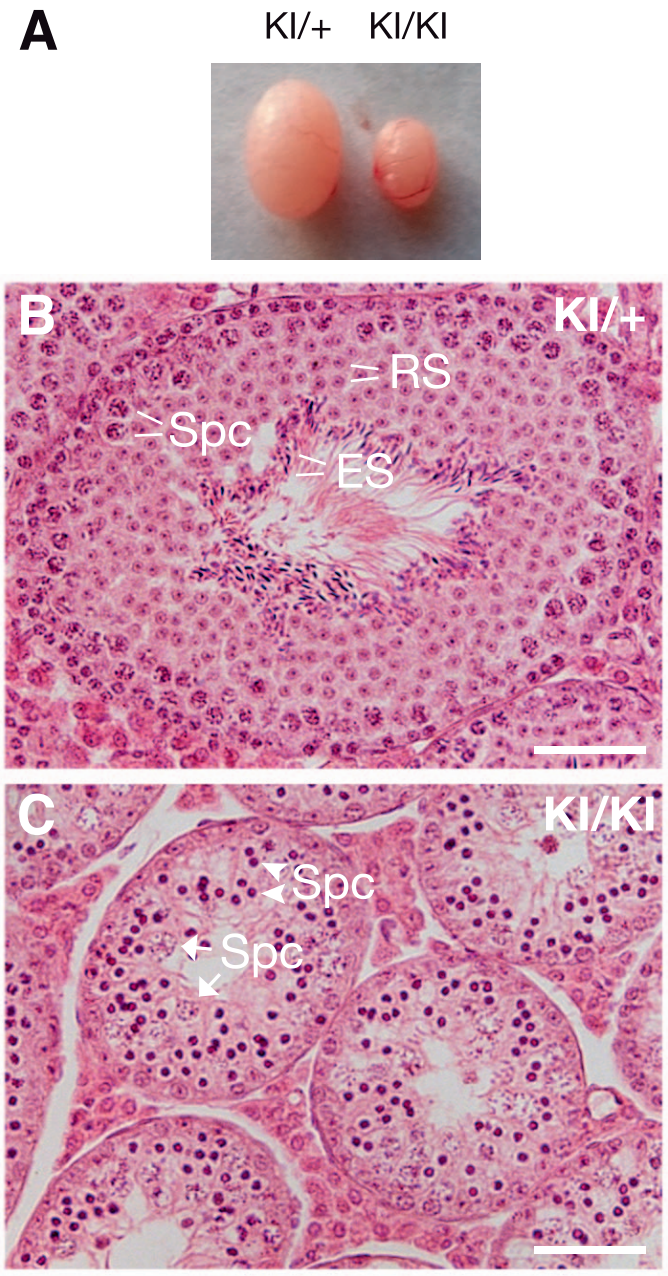

FIG. 2. Meiotic arrest in *Mov10l1*$^{KI/KI}$ mice. **A**) Dramatic size reduction of testis from 6-wk-old *Mov10l1*$^{KI/KI}$ mice. **B** and **C**) Histology of testes from 8-wk-old *Mov10l1*$^{KI/+}$ and *Mov10l1*$^{KI/KI}$ mice. Two types of spermatocytes are present in the *Mov10l1*$^{KI/KI}$ seminiferous tubules, indicated by arrowheads and arrows respectively. ES, elongating spermatids; RS, round spermatids; Spc, spermatocytes. Bars = 50 μm.

We examined histology of testes from adult *Mov10l1*$^{KI/+}$ and *Mov10l1*$^{KI/KI}$ mice to determine the effect of the *Mov10l1* ATP hydrolysis mutation on germ cell development. Spermatogenesis proceeded normally in the seminiferous tubules of *Mov10l1*$^{KI/+}$ mice (Fig. 2B). However, seminiferous tubules in *Mov10l1*$^{KI/KI}$ testes lacked any germ cells beyond the zygotene stage of meiosis I, showing that spermatogenesis is blocked in meiosis in the mutant males (Fig. 2C). Intriguingly, spermatocytes exhibited two types of nuclear morphology: one with strongly stained and condensed nuclei (Fig. 2C, arrowheads) and the other with loose and enlarged nuclei (Fig. 2C, arrows). In this new *Mov10l* knockin mutant, the ATP binding site was intact (Fig. 1A). Therefore, results from this mutant suggest that the ATP hydrolysis activity of MOV10L1 may also be required for spermatogenesis. Alternatively, the spermatogenic defect in this mutant could be caused by reduced MOV10L1 protein levels.

Piwi Proteins Are Depleted of piRNAs in Mov10l1$^{KI/KI}$ *Embryonic Germ Cells*

Meiotic arrest occurs as a result of a loss of pre-pachytene piRNAs. To determine whether mutation in the MOV10L1 ATP hydrolysis site affects the piRNA pathway, we assayed the loading of pre-pachytene piRNAs onto MILI and MIWI2 in the testes from E16.5 *Mov10l1*$^{KI/+}$ and *Mov10l1*$^{KI/KI}$ embryos. MILI- and MIWI2-bound piRNAs are 26-nucleotide (nt) and 28-nt long, respectively [12]. MILI- and MIWI2-bound piRNAs were present in E16.5 *Mov10l1*$^{KI/+}$ testes but absent in *Mov10l1*$^{KI/KI}$ testes (Fig. 3). This result suggests that the MOV10L1 ATP hydrolysis activity may be required for biogenesis or loading of pre-pachytene piRNAs. However, we cannot exclude the possibility that the failure in biogenesis or loading of pre-pachytene piRNAs might be caused by reduced MOV10L1 protein levels.

In the *Mov10l1*$^{KI/KI}$ testes, MILI was associated with small RNA species, one of which was 26 nt long (Fig. 3). The 26-nt band and larger RNA species were absent in the MIWI2 immunoprecipitation in the mutant. Deep sequencing of the RNAs associated with MILI in the *Mov10l1*$^{KI/KI}$ testes showed that these RNAs seemed to be random sequences, that is, they were neither piRNAs nor micro-RNAs. One possible explanation is that MILI, in the absence of its natural RNA substrate (piRNAs), simply binds to RNAs in a nonspecific manner.

De-repression of IAP and LINE1 Retrotransposons in Embryonic and Postnatal Mov10l1$^{KI/KI}$ *Germ Cells*

Because the main function of pre-pachytene piRNAs is to silence active transposable elements in the germline, we sought to address whether retrotransposon activity was affected in embryonic *Mov10l1*$^{KI/KI}$ germ cells. IAP and LINE1 are commonly de-repressed transposable elements in piRNA pathway mutants. We examined the expression of IAP and LINE1 in E16.5 *Mov10l1*$^{KI/+}$ and *Mov10l1*$^{KI/KI}$ testes by immunostaining for GAG and ORF1, proteins encoded by IAP and LINE1 retrotransposons, respectively [47, 48]. IAP and LINE1 were barely detectable in the E16.5 *Mov10l1*$^{KI/+}$ gonocytes, whereas they were significantly up-regulated in the *Mov10l1*$^{KI/KI}$ gonocytes (Fig. 4, A–D). LINE1 appeared to be more highly de-repressed than IAP. De-repression of retrotransposons in embryonic *Mov10l1*$^{KI/KI}$ germ cells is consistent with loss of pre-pachytene piRNAs.

We also analyzed the expression of IAP and LINE1 in 6-wk-old testes by immunofluorescence (Fig. 5). IAP and LINE1-encoded proteins were not readily detected in *Mov10l1*$^{KI/+}$ germ cells (Fig 5, A and C), but were significantly upregulated in germ cells from *Mov10l1*$^{KI/KI}$ testes (Fig. 5, B and D). In *Mov10l1*$^{KI/KI}$ testes, IAP was upregulated in spermatogonia, but not in spermatocytes (Fig. 5B); in contrast, LINE1 was upregulated in spermatocytes but not in spermatogonia (Fig. 5D). This binary de-repression pattern of IAP and LINE1 was previously observed in the *Mov10l1* knockout testes [16]. In addition, the binary LINE1 de-repression pattern was also reported in the *Mili* mutant and attributed to an additional requirement of histone H3 lysine 9 dimethylation in spermatogonia [53]. In conclusion, our *Mov10l1*$^{KI/KI}$ mutant exhibits de-repression of transposable elements in both embryonic and postnatal germ cells.

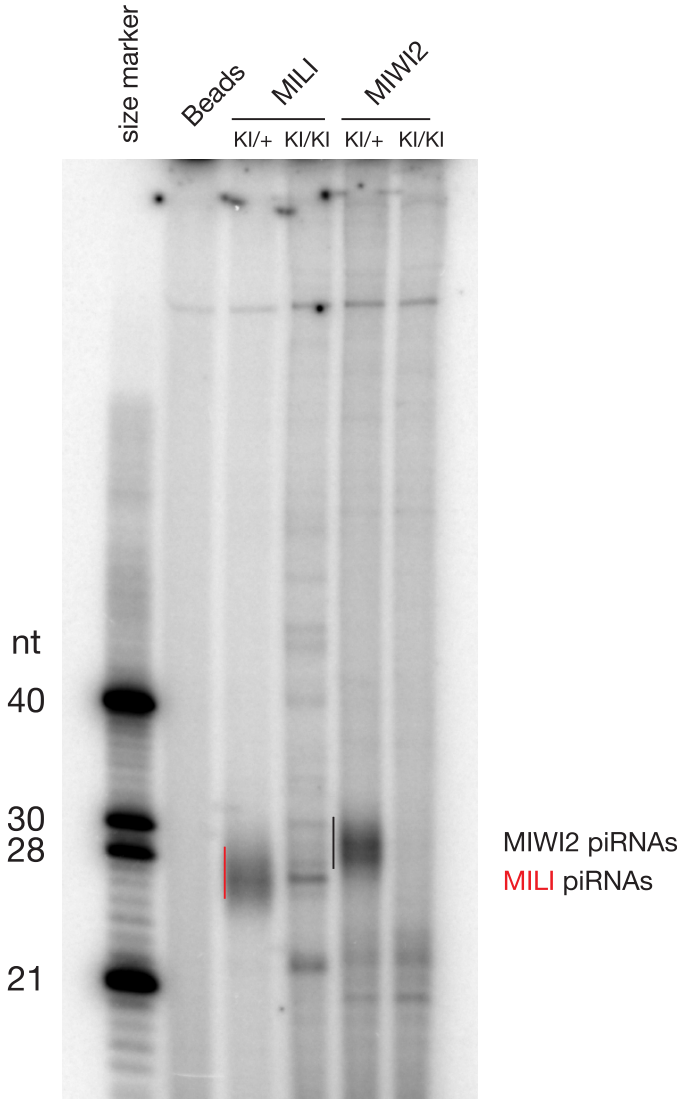

FIG. 3. MILI and MIWI2 are depleted of pre-pachytene piRNAs in embryonic *Mov10l1*$^{KI/KI}$ testes. The MILI and MIWI2 complexes were immunoprecipitated from the testes of E16.5 *Mov10l1*$^{KI/+}$ and *Mov10l1*$^{KI/KI}$ embryos. MILI-bound and MIWI2-bound RNAs (vertical lines) were isolated from MILI and MIWI2 complexes and radiolabeled for the detection of piRNAs. Lysate incubated with uncoupled beads served as a control. The RNAs associated with MILI in the *Mov10l1*$^{KI/KI}$ testes were sequenced using HiSeq 2000 platform for 50 cycles.

Polar Congregation of piRNA Pathway Proteins in Embryonic Mov10l1$^{KI/KI}$ *Gonocytes*

We next examined the localization of piRNA pathway proteins in E16.5 *Mov10l1*$^{KI/KI}$ testes. Pre-pachytene piRNAs are required to shuttle MIWI2 from the cytoplasm into the nucleus. In *Mili*$^{-/-}$ mice, piRNAs are not loaded onto MIWI2, and MIWI2 is excluded from the nucleus [12]. Nuclear exclusion of MIWI2 is common in other piRNA pathway mutants [8, 9]. We examined the subcellular localization of MIWI2 in testes from E16.5 *Mov10l1*$^{KI/+}$ and *Mov10l1*$^{KI/KI}$ embryos. As expected, MIWI2 localized predominantly to the nucleus of gonocytes in *Mov10l1*$^{KI/+}$ embryos, but was present only in the cytoplasm of gonocytes in *Mov10l1*$^{KI/KI}$ embryos (Fig. 6, A and B). Additionally, MIWI2 congregated in a polar granule in the cytoplasm of gonocytes in *Mov10l1*$^{KI/KI}$ embryos (Fig. 6B). We then examined the localization of two

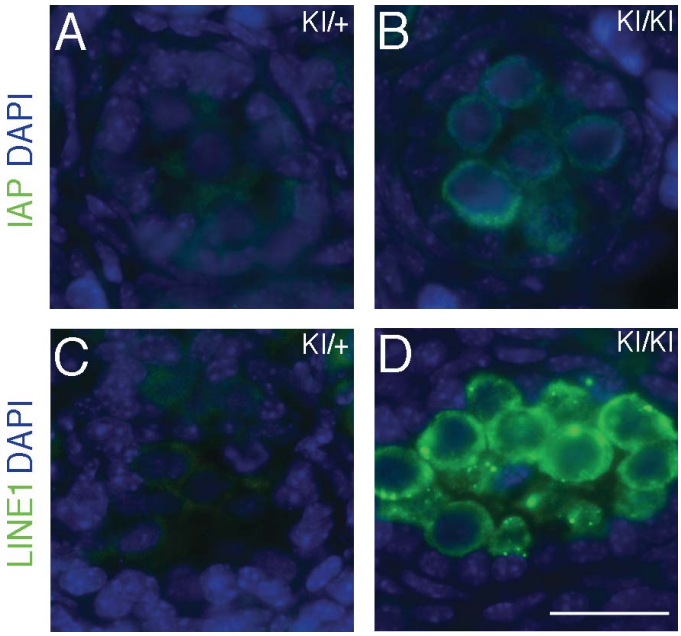

FIG. 4. De-repression of IAP and LINE1 retrotransposons in *Mov10l1*$^{KI/KI}$ gonocytes is shown. Sections of testes from E16.5 *Mov10l1*$^{KI/+}$ and *Mov10l1*$^{KI/KI}$ embryos were immunostained with antibodies against (**A** and **B**) IAP GAG and (**C** and **D**) LINE1 ORF1p. DNA was stained with DAPI. Bar = 50 μm.

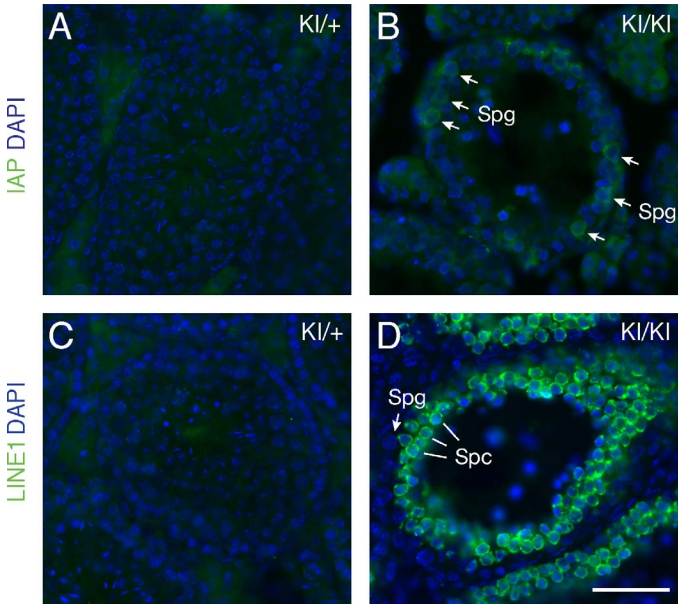

FIG. 5. De-repression of IAP and LINE1 retrotransposons in postnatal *Mov10l1*$^{KI/KI}$ testes is shown. Sections of testes from 6-wk-old *Mov10l1*$^{KI/+}$ and *Mov10l1*$^{KI/KI}$ mice were immunostained with antibodies against (**A** and **B**) IAP GAG and (**C** and **D**) LINE1 ORF1p. DNA was stained with DAPI. Spc, spermatocytes; Spg, spermatogonia. Bar = 50 μm.

other components (MILI and MOV10L1) in the piRNA pathway to determine if their localization was also affected in the E16.5 testes. MILI and MOV10L1 localized diffusely throughout the cytoplasm of *Mov10l1*$^{KI/+}$ gonocytes, but MILI and mutant MOV10L1 localized to one pole in the cytoplasm of *Mov10l1*$^{KI/KI}$ gonocytes in mice. These results show that localization of components of the piRNA pathway protein components is severely altered in embryonic *Mov10l1*$^{KI/KI}$ gonocytes.

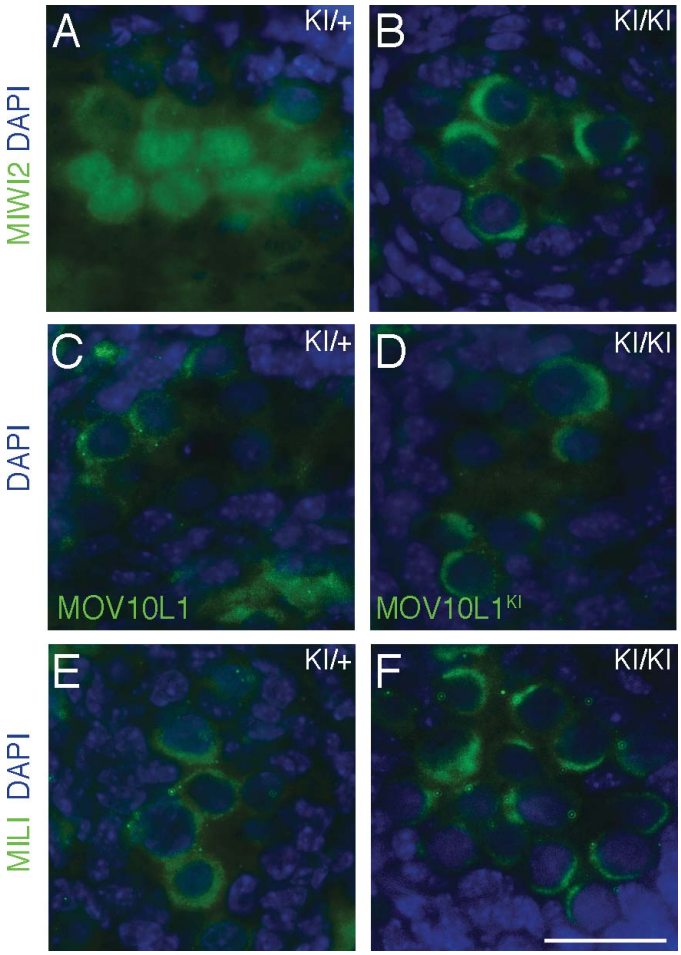

FIG. 6. piRNA pathway proteins form polar conglomeration in embryonic *Mov10l1*$^{KI/KI}$ gonocytes. Sections of testes from E16.5 *Mov10l1*$^{KI/+}$ and *Mov10l1*$^{KI/KI}$ embryos were immunostained with antibodies against MIWI2 (**A** and **B**), MOV10L1 (**C** and **D**), and MILI (**E** and **F**). DNA was stained with DAPI. Bar = 50 μm.

DISCUSSION

Here we examined the role of MOV10L1 ATP hydrolysis activity in piRNA biogenesis by using a genetic approach. Mutations in the MOV10L1 ATP hydrolysis motif resulted in a loss of pre-pachytene piRNAs. The MOV10L1 mutant protein was present in embryonic germ cells. Therefore, the molecular defects in embryonic germ cells could be attributed to the mutation of two conserved residues in the MOV10L1 ATP hydrolysis motif. However, as the abundance of MOV10L1 mutant protein was reduced, we could not exclude the possibility that the defects might be caused by reduced protein levels. Two additional *Mov10l1* mouse mutants were previously generated, in which the RNA helicase domain of MOV10L1 was deleted, and a point mutation was made in the MOV10L1 ATP-binding motif [16, 43]. These three *Mov10l1* mouse mutants exhibited the same phenotypes, loss of piRNAs, de-repression of transposable elements, meiotic arrest, and male sterility. Previous study of the ATP-binding site knockin mutant shows that the ATP-binding activity is required for piRNA biogenesis [43]. Study of the *Mov10l1* ATP hydrolysis knockin mutant generated here suggests that ATP binding may not be sufficient for piRNA biogenesis and that ATP hydrolysis may also be required. We hypothesize that ATP hydrolysis may provide the energy necessary for MOV10L1 to resolve secondary structures such as G-quadruplexes in the piRNA precursors.

The mutant MOV10L1 protein was not detected in postnatal testes from *Mov10l1*$^{KI/KI}$ mice with the mutation of two conserved residues in its ATP hydrolysis motif. In contrast, MILI was still expressed in early postnatal *Mov10l1*$^{KI/KI}$ testes. Therefore, it is unlikely that piRNA biogenesis is required for the stability of piRNA pathway proteins. Rather, the two residues (DE) that were mutated in the *Mov10l1* ATP hydrolysis site may be critical for MOV10L1 protein stability in postnatal testes. Intriguingly, the truncated MOV10L1 protein lacking part of the RNA helicase domain (including the DE residues) was present in postnatal testes from the previously generated mutant mice [16].

Polar congregation of piRNA pathway proteins has also been observed in other piRNA pathway mutants including *Pld6*, *Tdrd1*, *Ddx4*, and *Ngn3-Cre;Mov10l1* conditional mutant mice [18, 33, 34]. The polar conglomeration of piRNA pathway proteins in mutant germ cells is accompanied by abnormal formation/disappearance of nuages, and aggregation of mitochondria in *Pld6* and *Ngn-Cre;Mov10l1* mutants [18, 33, 34]. Both the nuage and the mitochondria are crucial to piRNA biogenesis. Although some piRNA pathway proteins such as MILI, TDRD1, MVH, and MOV10L1 are compartmentalized in the nuage, other piRNA pathway proteins including PLD6, PNLDC1, and TDRKH are mitochondrial proteins [8, 23, 40, 54]. The intricate interplay between nuage and mitochondria in piRNA biogenesis remains to be elucidated.

ACKNOWLEDGMENT

We thank J. Martinez and G. Hannon for MIWI2 antibody; S. L. Martin and A. Bortvin for LINE1 ORF1p antibody; B.R. Cullen for IAP GAG antibody; and R. Sachidanandam for help with sequence analysis.

REFERENCES

1. Batista PJ, Ruby JG, Claycomb JM, Chiang R, Fahlgren N, Kasschau KD, Chaves DA, Gu W, Vasale JJ, Duan S, Conte D, Jr, Luo S, et al. PRG-1 and 21U-RNAs interact to form the piRNA complex required for fertility in C. elegans. Mol Cell 2008; 31:67–78.
2. Chen PY, Manninga H, Slanchev K, Chien M, Russo JJ, Ju J, Sheridan R, John B, Marks DS, Gaidatzis D, Sander C, Zavolan M, et al. The developmental miRNA profiles of zebrafish as determined by small RNA cloning. Genes Dev 2005; 19:1288–1293.
3. Aravin AA, Naumova NM, Tulin AV, Vagin VV, Rozovsky YM, Gvozdev VA. Double-stranded RNA-mediated silencing of genomic tandem repeats and transposable elements in the *D. melanogaster* germline. Curr Biol 2001; 11:1017–1027.
4. Aravin A, Gaidatzis D, Pfeffer S, Lagos-Quintana M, Landgraf P, Iovino N, Morris P, Brownstein MJ, Kuramochi-Miyagawa S, Nakano T, Chien M, Russo JJ, et al. A novel class of small RNAs bind to MILI protein in mouse testes. Nature 2006; 442:203–207.
5. Girard A, Sachidanandam R, Hannon GJ, Carmell MA. A germline-specific class of small RNAs binds mammalian Piwi proteins. Nature 2006; 442:199–202.
6. Grivna ST, Beyret E, Wang Z, Lin H. A novel class of small RNAs in mouse spermatogenic cells. Genes Dev 2006; 20:1709–1714.
7. Siomi MC, Sato K, Pezic D, Aravin AA. PIWI-interacting small RNAs: the vanguard of genome defence. Nat Rev Mol Cell Biol 2011; 12:246–258.
8. Pillai RS. Chuma S. piRNAs and their involvement in male germline development in mice. Dev Growth Differ 2012; 54:78–92.
9. Fu Q, Wang PJ. Mammalian piRNAs: Biogenesis, function, and mysteries. Spermatogenesis 2014; 4:e27889.
10. Aravin AA, Sachidanandam R, Girard A, Fejes-Toth K, Hannon GJ. Developmentally regulated piRNA clusters implicate MILI in transposon control. Science 2007; 316:744–747.
11. Kuramochi-Miyagawa S, Watanabe T, Gotoh K, Totoki Y, Toyoda A, Ikawa M, Asada N, Kojima K, Yamaguchi Y, Ijiri TW, Hata K, Li E, et al. DNA methylation of retrotransposon genes is regulated by Piwi family members MILI and MIWI2 in murine fetal testes. Genes Dev 2008; 22: 908–917.

12. Aravin AA, Sachidanandam R, Bourc'his D, Schaefer C, Pezic D, Toth KF, Bestor T, Hannon GJ. A piRNA pathway primed by individual transposons is linked to de novo DNA methylation in mice. Mol Cell 2008; 31:785–799.
13. Carmell MA, Girard A, van de Kant HJ, Bourc'his D, Bestor TH, de Rooij DG, Hannon GJ. MIWI2 is essential for spermatogenesis and repression of transposons in the mouse male germline. Dev Cell 2007; 12:503–514.
14. Pezic D, Manakov SA, Sachidanandam R, Aravin AA. piRNA pathway targets active LINE1 elements to establish the repressive H3K9me3 mark in germ cells. Genes Dev 2014; 28:1410–1428.
15. De Fazio S, Bartonicek N, Di Giacomo M, Abreu-Goodger C, Sankar A, Funaya C, Antony C, Moreira PN, Enright AJ, O'Carroll D. The endonuclease activity of Mili fuels piRNA amplification that silences LINE1 elements. Nature 2011; 480:259–263.
16. Zheng K, Xiol J, Reuter M, Eckardt S, Leu NA, McLaughlin KJ, Stark A, Sachidanandam R, Pillai RS, Wang PJ. Mouse MOV10L1 associates with Piwi proteins and is an essential component of the Piwi-interacting RNA (piRNA) pathway. Proc Natl Acad Sci U S A 2010; 107:11841–11846.
17. Shoji M, Tanaka T, Hosokawa M, Reuter M, Stark A, Kato Y, Kondoh G, Okawa K, Chujo T, Suzuki T, Hata K, Martin SL, et al. The TDRD9-MIWI2 complex is essential for piRNA-mediated retrotransposon silencing in the mouse male germline. Dev Cell 2009; 17:775–787.
18. Watanabe T, Chuma S, Yamamoto Y, Kuramochi-Miyagawa S, Totoki Y, Toyoda A, Hoki Y, Fujiyama A, Shibata T, Sado T, Noce T, Nakano T, et al. MITOPLD is a mitochondrial protein essential for nuage formation and piRNA biogenesis in the mouse germline. Dev Cell 2011; 20:364–375.
19. Kuramochi-Miyagawa S, Kimura T, Ijiri TW, Isobe T, Asada N, Fujita Y, Ikawa M, Iwai N, Okabe M, Deng W, Lin H, Matsuda Y, et al. Mili, a mammalian member of piwi family gene, is essential for spermatogenesis. Development 2004; 131:839–849.
20. Tanaka SS, Toyooka Y, Akasu R, Katoh-Fukui Y, Nakahara Y, Suzuki R, Yokoyama M, Noce T. The mouse homolog of *Drosophila* Vasa is required for the development of male germ cells. Genes Dev 2000; 14:841–853.
21. Soper SF, van der Heijden GW, Hardiman TC, Goodheart M, Martin SL, de Boer P, Bortvin A. Mouse maelstrom, a component of nuage, is essential for spermatogenesis and transposon repression in meiosis. Dev Cell 2008; 15:285–297.
22. Ma L, Buchold GM, Greenbaum MP, Roy A, Burns KH, Zhu H, Han DY, Harris RA, Coarfa C, Gunaratne PH, Yan W, Matzuk MM. GASZ is essential for male meiosis and suppression of retrotransposon expression in the male germline. PLoS Genet 2009; 5:e1000635.
23. Saxe JP, Chen M, Zhao H, Lin H. Tdrkh is essential for spermatogenesis and participates in primary piRNA biogenesis in the germline. EMBO J 2013; 32:1869–1885.
24. van der Heijden GW, Bortvin A. Transient relaxation of transposon silencing at the onset of mammalian meiosis. Epigenetics 2009; 4:76–79.
25. Yang F, Wang PJ. Multiple LINEs of retrotransposon silencing mechanisms in the mammalian germline. Semin Cell Dev Biol (in press). Published online ahead of print 5 March 2016 as DOI: 10.1016/j.semcdb.2016.03.001.
26. Li XZ, Roy CK, Dong X, Bolcun-Filas E, Wang J, Han BW, Xu J, Moore MJ, Schimenti JC, Weng Z, Zamore PD. An ancient transcription factor initiates the burst of piRNA production during early meiosis in mouse testes. Mol Cell 2013; 50:67–81.
27. Goh WS, Falciatori I, Tam OH, Burgess R, Meikar O, Kotaja N, Hammell M. Hannon GJ. piRNA-directed cleavage of meiotic transcripts regulates spermatogenesis. Genes Dev 2015; 29:1032–1044.
28. Gou LT, Dai P, Yang JH, Xue Y, Hu YP, Zhou Y, Kang JY, Wang X, Li H, Hua MM, Zhao S, Hu SD, et al. Pachytene piRNAs instruct massive mRNA elimination during late spermiogenesis. Cell Res 2014; 24:680–700.
29. Zhang P, Kang JY, Gou LT, Wang J, Xue Y, Skogerboe G, Dai P, Huang DW, Chen R, Fu XD, Liu MF, He SMIWI. and piRNA-mediated cleavage of messenger RNAs in mouse testes. Cell Res 2015; 25:193–207.
30. Di Giacomo M, Comazzetto S, Saini H, De Fazio S, Carrieri C, Morgan M, Vasiliauskaite L, Benes V, Enright AJ, O'Carroll D. Multiple epigenetic mechanisms and the piRNA pathway enforce LINE1 silencing during adult spermatogenesis. Mol Cell 2013; 50:601–608.
31. Reuter M, Berninger P, Chuma S, Shah H, Hosokawa M, Funaya C, Antony C, Sachidanandam R, Pillai RS. Miwi catalysis is required for piRNA amplification-independent LINE1 transposon silencing. Nature 2011; 480:264–267.
32. Deng W, Miwi, Lin H. A murine homolog of Piwi encodes a cytoplasmic protein essential for spermatogenesis. Dev Cell 2002; 2:819–830.
33. Zheng K, Wang PJ. Blockade of pachytene piRNA biogenesis reveals a novel requirement for maintaining post-meiotic germline genome integrity. PLoS Genet 2012; 8:e1003038.
34. Chuma S, Hosokawa M, Kitamura K, Kasai S, Fujioka M, Hiyoshi M, Takamune K, Noce T, Nakatsuji N. Tdrd1/Mtr-1, a tudor-related gene, is essential for male germ-cell differentiation and nuage/germinal granule formation in mice. Proc Natl Acad Sci U S A 2006; 103:15894–15899.
35. Aravin AA, van der Heijden GW, Castaneda J, Vagin VV, Hannon GJ, Bortvin A. Cytoplasmic compartmentalization of the fetal piRNA pathway in mice. PLoS Genet 2009; 5:e1000764.
36. Meikar O, Da Ros M, Korhonen H, Kotaja N. Chromatoid body and small RNAs in male germ cells. Reproduction 2011; 142:195–209.
37. Ipsaro JJ, Haase AD, Knott SR, Joshua-Tor L, Hannon GJ. The structural biochemistry of zucchini implicates it as a nuclease in piRNA biogenesis. Nature 2012; 491:279–283.
38. Nishimasu H, Ishizu H, Saito K, Fukuhara S, Kamatani MK, Bonnefond L, Matsumoto N, Nishizawa T, Nakanaga K, Aoki J, Ishitani R, Siomi H, et al. Structure and function of Zucchini endoribonuclease in piRNA biogenesis. Nature 2012; 491:284–287.
39. Vourekas A, Zheng Q, Alexiou P, Maragkakis M, Kirino Y, Gregory BD, Mourelatos Z. Mili and Miwi target RNA repertoire reveals piRNA biogenesis and function of Miwi in spermiogenesis. Nat Struct Mol Biol 2012; 19:773–781.
40. Izumi N, Shoji K, Sakaguchi Y, Honda S, Kirino Y, Suzuki T, Katsuma S, Tomari Y. Identification and functional analysis of the Pre-piRNA 3′ trimmer in silkworms. Cell 2016; 164:962–973.
41. Kawaoka S, Izumi N, Katsuma S, Tomari Y. 3′ end formation of PIWI-interacting RNAs in vitro. Mol Cell 2011; 43:1015–1022.
42. Lim SL, Qu ZP, Kortschak RD, Lawrence DM, Geoghegan J, Hempfling AL, Bergmann M, Goodnow CC, Ormandy CJ, Wong L, Mann J, Scott HS, et al. HENMT1 and piRNA stability are required for adult male germ cell transposon repression and to define the spermatogenic program in the mouse. PLoS Genet 2015; 11:e1005620.
43. Vourekas A, Zheng K, Fu Q, Maragkakis M, Alexiou P, Ma J, Pillai RS, Mourelatos Z, Wang PJ. The RNA helicase MOV10L1 binds piRNA precursors to initiate piRNA processing. Genes Dev 2015; 29:617–629.
44. Lewandoski M, Martin GR. Cre-mediated chromosome loss in mice. Nat Genet 1997; 17:223–225.
45. Reuter M, Chuma S, Tanaka T, Franz T, Stark A, Pillai RS. Loss of the Mili-interacting Tudor domain-containing protein-1 activates transposons and alters the Mili-associated small RNA profile. Nat Struct Mol Biol 2009; 16:639–646.
46. Pandey RR, Tokuzawa Y, Yang Z, Hayashi E, Ichisaka T, Kajita S, Asano Y, Kunieda T, Sachidanandam R, Chuma S, Yamanaka S, Pillai RS. Tudor domain containing 12 (TDRD12) is essential for secondary PIWI interacting RNA biogenesis in mice. Proc Natl Acad Sci U S A 2013;
47. Martin SL, Branciforte D. Synchronous expression of LINE-1 RNA and protein in mouse embryonal carcinoma cells. Mol Cell Biol 1993; 13: 5383–5392.
48. Bogerd HP, Wiegand HL, Doehle BP, Lueders KK, Cullen BR. APOBEC3A and APOBEC3B are potent inhibitors of LTR-retrotransposon function in human cells. Nucleic Acids Res 2006; 34:89–95.
49. Fairman-Williams ME, Guenther UP, Jankowsky E. SF1 and SF2 helicases: family matters. Curr Opin Struct Biol 2010; 20:313–324.
50. Weng Y, Czaplinski K, Peltz SW. Genetic and biochemical characterization of mutations in the ATPase and helicase regions of the Upf1 protein. Mol Cell Biol 1996; 16:5477–5490.
51. Story RM, Steitz TA. Structure of the recA protein-ADP complex. Nature 1992; 355:374–376.
52. Walker JE, Saraste M, Runswick MJ, Gay NJ. Distantly related sequences in the alpha- and beta-subunits of ATP synthase, myosin, kinases and other ATP-requiring enzymes and a common nucleotide binding fold. EMBO J 1982; 1:945–951.
53. Di Giacomo M, Comazzetto S, Sampath SC, Sampath SC, O'Carroll D. G9a co-suppresses LINE1 elements in spermatogonia. Epigenetics Chromatin 2014; 7:24.
54. Zheng K, Wu X, Kaestner KH, Wang PJ. The pluripotency factor LIN28 marks undifferentiated spermatogonia in mouse. BMC Dev Biol 2009; 9:38.